The numerical investigation of human micro-climate with different human simulators

Haruna Yamasawa*[1], Sung-Jun Yoo [2], Kazuki Kuga[2], and Kazuhide Ito[2]

1 Osaka University
2-1, Yamadaoka
Suita, Osaka, Japan
**Corresponding and presenting author:*
yamasawa@arch.eng.osaka-u.ac.jp

2 Kyushu University
6-1, Kasuga-koen, Kasuga-city
Fukuoka, Japan

ABSTRACT

The development of computational fluid dynamics (CFD) made it possible to simulate the detailed flow field and temperature field within the room. The various studies numerically investigated the flow and temperature field both inside and outside the buildings. When investigating the indoor environment, human is an important factor since it perceives the indoor environment and behaves as a source of heat and contaminant as well. Some studies investigated deeper into humans by developing detailed computer-simulated persons (CSP). However, due to the limitation of computer performance, it is still not always possible to conduct the simulation with detailed CSPs. Therefore, many studies adopted the human simulators with simplified geometry, e.g., cylinder and cuboid. However, it is necessary to understand the effect of the geometrical difference of human simulators on the simulation results. Therefore, CFD analysis with different human simulator geometry is conducted to understand the effect.
A human simulator is located in the middle of a room (3 x 3 x 3 m) with an inlet at a lower level of the room and an outlet at a higher level of the room. The air of 20 °C flows into the room via inlet boundary condition with the air velocity of 0.1 m/s. The human simulator geometry is the parameter in this study, and the studied cases are cuboid, simplified CSP, and detailed CSP. The Fanger model is applied for simulating heat generation from human skin surface; therefore, the heat generation rate differs depending on the conditions.
As a result, it was shown that the total heat generation rate and surface temperature of human simulators are almost the same, therefore, since all other walls are insulated, the exhaust air temperature also did not differ depending on the cases. However, there was some difference in the ratio between convective and radiative heat loss through the skin. In addition, although the heat generation rate is almost the same, the flow rate of thermal plume around them differed by 10% depending on the human simulator geometry.

KEYWORDS

Computer simulated person, Heat generation rate, Thermal plume, CFD analysis, Human simulator

1 INTRODUCTION

The development of computational fluid dynamics (CFD) made it possible to simulate the detailed flow field and temperature field within the room. The various studies numerically investigated the flow and temperature field both inside and outside the buildings. When investigating the indoor environment, human is an important factor since it perceives the indoor environment and behaves as a source of heat and contaminant as well. Some studies (Nielsen et al., 2003; Takada et al., 2016; Yoo & Ito, 2018, 2022) investigated deeper into humans by developing detailed computer-simulated persons (CSP). However, due to the limitation of computer performance, it is still not always possible to conduct the simulation with detailed CSPs. Therefore, many studies adopted the human simulators with simplified geometry, e.g., cylinder and cuboid (Lau & Chen, 2007; Yuan et al., 1999). However, it is necessary to understand the effect of the geometrical difference of human simulators on the simulation results. Therefore, to understand the effect of geometrical difference in human simulator, CFD analysis with different human simulator geometry is conducted.

2 METHODOLOGY: HUMAN SIMULATOR

The geometries of the human simulators that simulating an adult male are shown in Fig. 1, and the surface areas of the human simulators are summarised in Table 1. The studied human simulators are as follows: i) cuboid with a dimensions of 0.25 x 0.25 x 1.8 m; ii) cuboid with a dimensions of 0.15 x 0.35 x 1.8 m; iii) angular human simulator that has a head and legs; iv) detailed CSP. The model geometries were decided by fixing the human body height to be almost the same as that of *Model CSP-detailed*, i.e., 1.8 m height. The body surface area was adjusted to be around the same as that of *Model CSP-detailed* as well. The surface area of each simplified models is kept within the range of 3% from that of *Model CSP-detailed*.

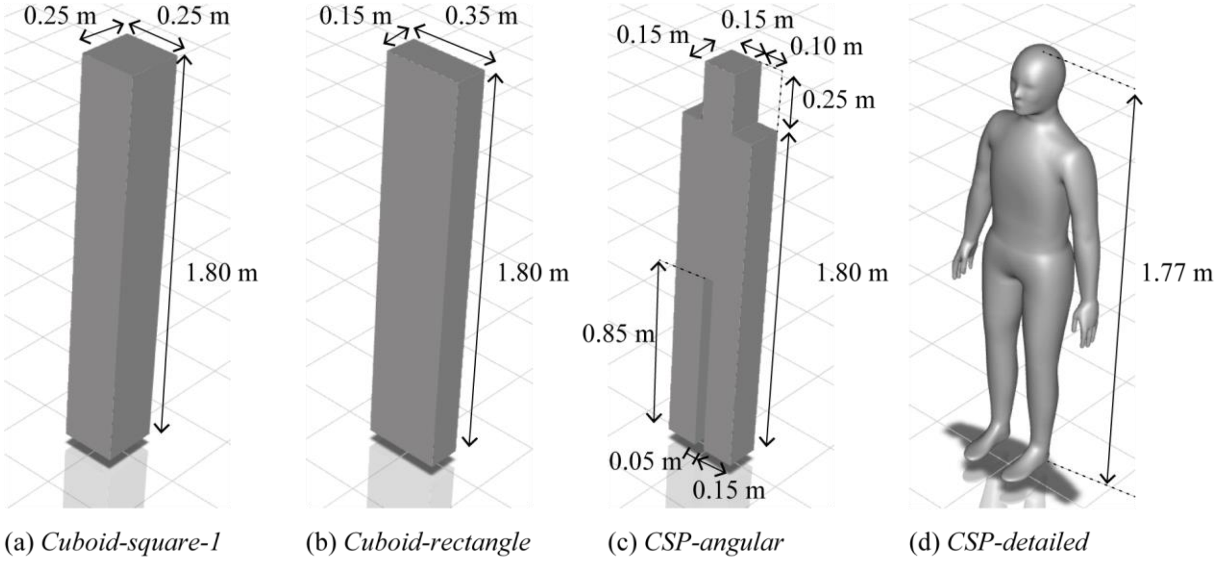

Figure 1: Geometries of the human simulators

Table 1: Geometrical information of the human simulators

Geometry	Surface area [m^2]	Height [m]	Number of cells
Cuboid-square	1.84 (-1.1%)	1.80	2,114,952
Cuboid-rectangle	1.83 (-1.6%)	1.80	2,064,930
CSP-angular	1.91 (+2.7%)	1.80	5,705,792
CSP-detailed	1.86 (Reference)	1.77	1,196,755

To investigate the difference of thermal plumes from each human simulators, skin surface temperature was controlled by adopting the Fanger's model (Fanger, 1972) to the boundary condition. The heat generation from the human simulators is expressed by the combination of core temperature and heat conductance through the core to the skin through the body. By using the simplified equations based on the Fanger's comfort equation (Fanger, 1972), the correlation between skin surface temperature T_{skin} and sensible heat generation from skin surface Q_{skin-s} can be expressed as follows:

$$Q_{skin-s} = 18.5 \times (36.4 - T_{skin}) \tag{1}$$

where, core temperature of the human body is set to be 36.4 ℃ and heat conductance between core of the body and the skin surface is set to be 18.5 W/m^{2}K.

3 METHODOLOGY: ANALYTICAL METHOD

The analytical domain and the studied cases are illustrated in Figure 2. Each human simulator is located at the middle of the room with a dimensions of 3 x 3 x 3 m. The cooled air is supplied to the room through an inlet located near the floor at a wall, and is exhausted from the room through an outlet located near the ceiling at the opposite wall. Both inlet and outlet have a dimension of 0.3 x 0.3 m. Due to the detailed geometry of *Model CSP-detailed*, two cases are studied for this model: the case that (a) air inflows through the inlet at the back and outflows through the outlet at the front, and (b) air inflows through the inlet at the back and outflows through the outlet at the front.

The simulation is conducted under non-isothermal condition using commercial software, Ansys Fluent. SST $k-\omega$ model is adopted, radiative heat transfer is calculated using S2S (Surface-to-surface) model, and the second-order upwind discretization scheme is adopted.

The boundary conditions are summarized in Table 2, and the number of cells in each model are summarised in Table 1. The cells around *Model CSP-detailed* is consist of unstructured meshes, whereas the other models are consisting of structured meshes due to their simplified geometry.

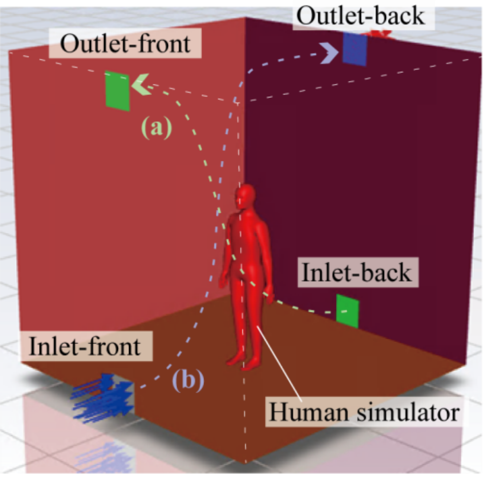

(a) Analytical room (Model CSP-detailed)

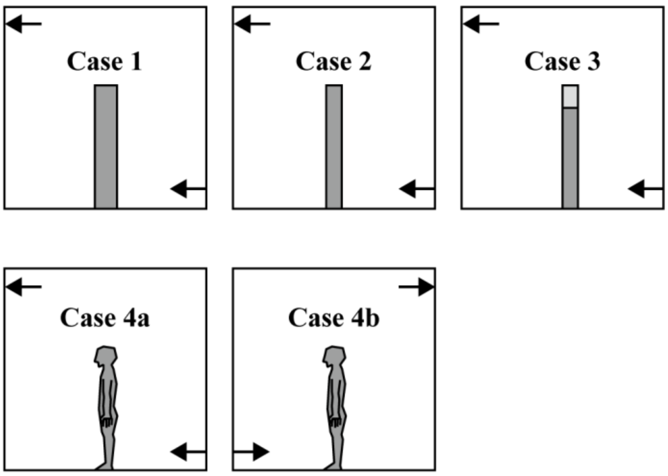

(b) Studied cases

Figure 2: Geometrical configuration of studied cases

Table 2: Boundary conditions

Inlet	Velocity: 0.1 m/s, Temperature: 20.0 °C
Outlet	Gradient zero
Wall	No slip, External emissivity: 0.95, Temperature: Gradient zero
Human skin surface	No slip, External emissivity: 0.98, Temperature: Calculated by Eq. (1)

4 RESULTS AND DISCUSSIONS

The exhaust air temperature and the mean temperature of skin surface are summarized in Table 3. There is no significant difference among all the cases in terms of exhaust temperature and mean skin temperature.

Table 3: Temperature results

Case	Geometry	*Exhaust temperature* [°C]	*Mean skin temperature* [°C]	Surface area [m^2]
1	Cuboid-square	28.5	33.7	1.84
2	Cuboid-rectangle	28.5	33.6	1.83
3	CSP-angular	28.5	33.8	1.91
4a	CSP-detailed (Flow: back-to-front)	28.5	33.7	1.86
4b	CSP-detailed (Flow: front-to-back)	28.2	33.7	1.86

Figure 3 and Figure 4 illustrates the heat flux and heat generation from human simulators, respectively. The total sensible heat flux and heat are almost the same among all the cases, i.e., 49 to 51 W/m^2 and 92 to 94 W. However, it must be noted that the ratio between radiative and convective heat transfer from the skin was different. Figure 5 illustrates the ratio between radiative and convective heat transfer from human simulator's skin. It is shown that the heat transfer by radiation is almost double of that by convection. In addition, it is shown that the radiative component is relatively small in Case-3 and Case-4, if compared to that in Case-1 and Case-2. It is assumed to be due the reproduction of the detailed geometries; the radiative heat transfer from skin surface only goes to the surrounding cooled walls in Case-1 and Case-2, whereas the radiative heat transfer also occurs between skin surfaces in Case-3 and Case-4. Therefore, due to the simplicity of the geometry, the radiative heat transfer is assumed to be overestimated (and convective heat transfer is underestimated) in cuboid human simulators.

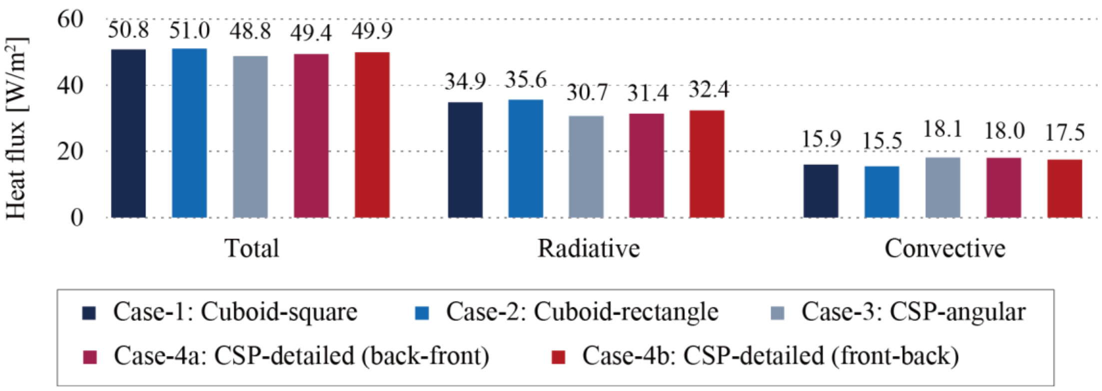

Figure 3: Heat flux from human simulators

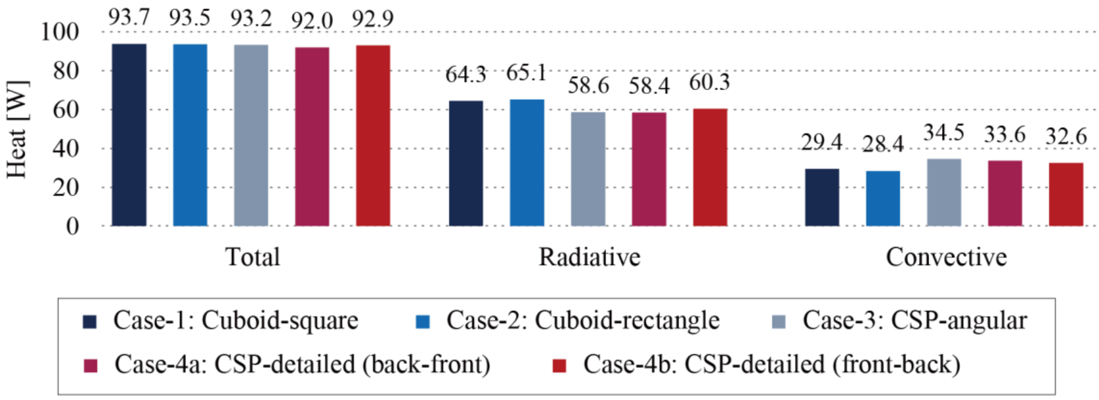

Figure 4: Heat from human simulators

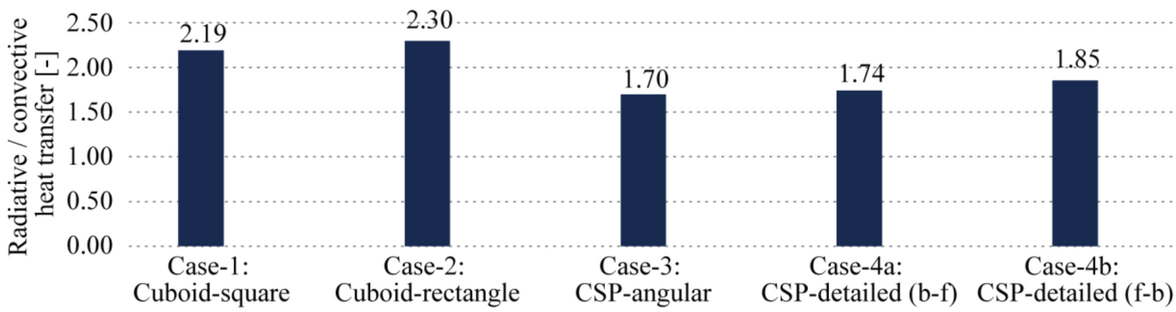

Figure 5: Ratio between radiative and convective heat transfer from human simulators

The thermal plume flow rate is shown in Figure 6. The thermal plume flow rate was calculated by conducting mass-weighted integral of upward air velocity around the human simulators. It must be noted that the velocity was integrated within the region that the upward air velocity is larger than 0.05 m/s. The plume flow rates in Case-1 and Case-2 are relatively small if compared to the other cases. It is because the convective component of heat transfer from cuboid human simulators are assumed to be underestimated as mentioned prior, which leads to the smaller drive force of the thermal plume. Moreover, it is assumed that the turbulence generated around the hip joint, also enhanced the increase of the flow rate. Additionally, the thermal plume flow rates of Case-4a and Case-4b are not identical to each other. It is suggested that more the human simulator's geometry is detailed, more the thermal plume flow rate is difficult to be simply predicted.

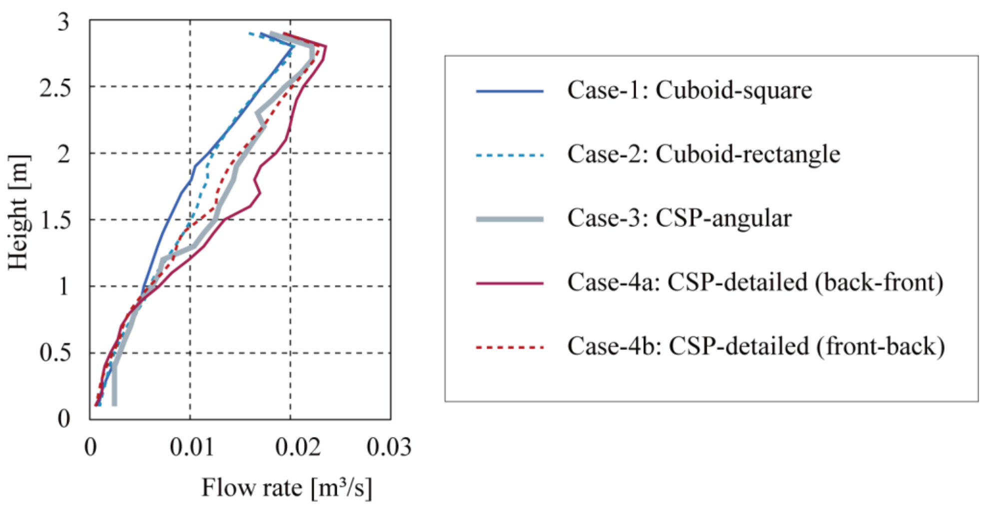

Figure 6: Plume flow rate from human simulators

5 CONCLUSIONS

To understand the effect of reproduction of the human simulators, CFD analysis was conducted with four different geometries of human simulators. The studied cases are: two kinds of cuboids, one simple CSP, and one detailed CSP. Each of the human simulators is located at the middle of the room (3 x 3 x 3 m), and the cooled air is supplied around the floor and is exhausted around the ceiling. As for the detailed CSP, two cases are conducted; (a) when air is supplied from the front, and (b) when air is supplied from the back.

It is shown that although the total sensible heat generation is almost the same among all the cases, however, the ratio between radiative and convective heat transfer differed. This also led to the difference in thermal plume flow rate.

6 ACKNOWLEDGEMENTS

This research was partially funded by the Japan Society for the Promotion of Science (JSPS) Grants-in-Aid for Scientific Research (KAKENHI) (grant numbers JP 22K18300, JP 22H00237, JP22J00743, JP22K14371, and JP 20KK0099), the Japan Science and Technology (JST), CREST Japan (grant number JP 20356547), FOREST program from JST, Japan (Grant number JPMJFR225R), and MEXT as "Program for Promoting Researches on the Supercomputer Fugaku" (JPMXP1020210316).

7 REFERENCES

Fanger, P. O. (1972). Thermal comfort: Analysis and applications in environmental engineering. *Applied Ergonomics*, *3*(3), 181. https://doi.org/10.1016/S0003-6870(72)80074-7

Lau, J., & Chen, Q. (2007). Floor-supply displacement ventilation for workshops. *Building and Environment*, *42*(4), 1718–1730. https://doi.org/10.1016/j.buildenv.2006.01.016

Nielsen, P., Murakami, S., Kato, S., Topp, C., & Yang, J.-H. (2003). Benchmark tests for a computer simulated person. *Aalborg University, …*, *October*, 1–6. http://homes.civil.aau.dk/pvn/cfd-benchmarks/csp_benchmark_test/Benchmark Tests_071103.pdf

Takada, S., Sasaki, A., & Kimura, R. (2016). Fundamental study of ventilation in air layer in clothing considering real shape of the human body based on CFD analysis. *Building and Environment*, *99*, 210–220. https://doi.org/10.1016/j.buildenv.2016.01.028

Yoo, S. J., & Ito, K. (2018). Assessment of transient inhalation exposure using in silico human model integrated with PBPK-CFD hybrid analysis. *Sustainable Cities and Society*, *40*(April), 317–325. https://doi.org/10.1016/j.scs.2018.04.023

Yoo, S. J., & Ito, K. (2022). Validation, verification, and quality control of computational fluid dynamics analysis for indoor environments using a computer-simulated person with respiratory tract. *Japan Architectural Review*, *5*(4), 714–727. https://doi.org/10.1002/2475-8876.12301

Yuan, X., Chen, Q., Glicksman, L. R., Hu, Y., & Yang, X. (1999). Measurements and computations of room airflow with displacement ventilation. *ASHRAE Transaction*, *105*, 340–352.